Journal of Applied Polymer Science

Development of Electromagnetic Interference Shielding Materials from the Composite of Nanostructured Polyaniline-Polyhydroxy Iron-Clay and Polycarbonate

Viswan Lilly Reena, Janardhanan Devaki Sudha, R. Ramakrishnan
Chemical Sciences and Technology Division, National Institute for Interdisciplinary Science and Technology, CSIR, Thiruvananthapuram 695019, India
Correspondence to: J. D. Sudha (E-mail: sudhajd2001@yahoo.co.in)

ABSTRACT: In the present study, we demonstrate the development of novel electromagnetic interference shielding material from the composite of nanostructured polyaniline-polyhydroxy iron-clay and polycarbonate through solution blending process. Onset of percolation threshold has been manifested from the morphological studies in combination with electrical conductivity measurements. Temperature-dependent electrical conduction mechanism was studied by applying Mott theory and was found to follow 3D variable range hopping (VRH) model. The presence of interaction between the host matrix and the nanofiller was studied by rheological property measurement in combination with Fourier transform infrared spectroscopy. Films were further characterized for electromagnetic interference (EMI) shielding efficiency and thermomechanical properties. Results suggest that these transparent composite films can be used for the fabrication of EMI shielding/electrostatic dissipation material for the encapsulation of electronic devices and as electrostatic material for high technological applications. © 2012 Wiley Periodicals, Inc. J. Appl. Polym. Sci. 000: 000–000, 2012

KEYWORDS: blending; conducting polymers; dispersions; microscopy; emulsion polymerization

Received 1 September 2011; accepted 6 July 2012; published online
DOI: 10.1002/app.38320

INTRODUCTION

Nanostructured multifunctional electromagnetic composites have attracted a great deal of attention for their potential applications in various fields such as electromagnetic interference (EMI) shielding, antistatic coatings, chemical sensors, transducers, and corrosion protection coatings.[1–6] EMI shielding essentially depends on the conductivity, dielectric constant, and magnetic property of the materials for various applications. It is known that the conducting material can effectively shield electromagnetic waves generated from an electric source, whereas magnetic materials can shield effectively the electromagnetic waves originated from a magnetic source. Thus, materials having dual property of conductivity and magnetic properties are suitable for EMI shielding applications. High thermomechanical properties are also expected for electromagnetic materials for high technological applications. Moreover, according to the electromagnetic wave theory, if the dimension of the conductive filler is in a nanometer regime and retains a high aspect ratio, it easily forms a conductive network at low concentration of the filler with high mechanical strength. Thus, the preparation of nanostructured polyaniline-polyhydroxy iron-clay (PPIC) composite is important as it is a novel guest–host system consisting of exfoliated/intercalated nanoclay layers having high aspect ratio, dispersed in nanomagnets encapsulated conducting PANI and is composed of electric, magnetic, and thermomechanical property in a unique material system. But the problem with these materials is its cost and low processability. To make EMI shielding products viable, composites have been fabricated by blending them with compatible and mechanically sound conventional polymers.[7,8]

The commodity polymer poly(bisphenol A carbonate) is receiving great attraction for the fabrication of composite for high technological applications because of its excellent processability, transparency, mechanical properties, good thermal stability, and good adhesion to other materials.[5] Electrically conductive composites of polycarbonate (PC) with conducting polymers such as PANI and PPy are interesting as they can exhibit low percolation threshold concentration arising from hydrogen bonding interaction between these two polymers.[9–11] Several strategies are reported for blending conducting polymers with conventional polymers which include solution blending, melt blending, and so on.[12] Apart from these, our group have used a one-step

surfactant micelle-induced emulsion polymerization strategy for the preparation of conductive composite of polyaniline-clay nanocomposite and polystyrene (PS) using the amphiphilic dopant 3-PDPSA.[13,14] They reported that the amphiphilic dopant could micellize PS matrix and the soft micelle could act as a structure directing agent to form electrically conductive blends of highly oriented nano-cylindrical PANI-dispersed PS. There are many reports on the use of functionalized protonic acids to dope PANI EB to improve its processability.[15] These functionalized acids having long alkyl chains can increase the solubility of PPIC in common organic solvents and can induce compatibility through plasticization with other polymer matrices.[16]

The EMI attenuation offered by a shield may depend on three mechanisms: the reflection of the wave from the shield, the absorption of the wave as it passes through the shield, and the multiple reflections of the waves at various surfaces or interfaces within the shield. The multiple reflections, however, requires the presence of large surface areas (e.g., a porous or foam material) or interface areas (e.g., a composite material containing fillers that have large surface area) in the shield. Thus, the composite prepared with PPIC and PC is expected to effectively shield the electromagnetic radiations.

Thus, the objective of the present study is to prepare composite films of nanostructured electromagnetic PPIC in PC matrix through solution blending. The prepared blends were characterized for electrical conductivity, temperature-dependent electrical conduction mechanism, percolation threshold concentration, rheological property, and morphology, EMI shielding efficiency, and thermomechanical properties.

EXPERIMENTAL

Materials and Methods

Aniline monomer (99.5% pure, Ranbaxy Chemicals, Mumbai) was distilled under reduced pressure. Ammonium persulphate (APS), methyl alcohol, and ferric chloride hexahydrate were purchased from S.D. Fine Chem, Mumbai, India, and were used without further purification. Sodium carbonate was purchased from Ranbaxy Fine Chemicals, India. Na^+ Cloisite clay with cation exchange capacity of 92.6 meq/100 g and a mean chemical formula of $(Na, Ca)_{0.33}(Al_{1.67}Mg_{0.33})Si_4O_{10}(OH).\ 2nH_2O$ was purchased from southern clay products. 3-Pentadecyl phenol-4-sulphonic acid (3-PDPSA) was prepared from 3-pentadecyl phenol (cardanol), obtained by the double distillation of cashew nut shell liquid (cashew export promotion council, India) at 3–4 mmHg at 230–235°C. PC was purchased from GE plastics, India. ($M_w = 50{,}000$ g/mol, glass transition temperature [T_g] = 150°C).

Preparation of PPIC Composites

The polyhydroxy iron cation (PIC) solution was prepared by the hydrolysis of 0.2*M* ferric chloride hexahydrate solution with sodium carbonate.[17] Typical synthetic procedure for the preparation of PPIC is as follows. PIC (11.5 mL, 0.2*M*) was added dropwise to 3-PDPSA ($10^{-3}M$, 25 mL) with stirring for 1 h. Aqueous suspension of clay (1 wt %) was added to the above vigorously stirring solution. The ratio of the cation to clay was 90 mmol/meq. Upon the complete addition of clay to the hydrolyzed Fe^{3+} solution, the reaction mixture was ultrasonicated for 2 h. Aniline (2.5 g) in 25 mL of water was then added and continued ultrasonication for another 0.5 h. Aniline : PDPSA mole ratio was kept at 1 : 0.1. Aqueous solution of APS (6.1 g in 60 mL water) was added to the above mixture and the resulting solution was stirred for another 5 min to ensure complete mixing. The reaction was continued without further agitation for 24 h at room temperature. Finally, the product was precipitated with methanol, washed with deionized water until the filtrate become colorless, and dried under vacuum at 60–80°C for 12 h.

Preparation of Electromagnetic Blends PPIC/PC

Electrically conductive blends of PPPC were prepared via solution blending. Stock solutions of PPIC (5% w/v) and PC (5% w/v) in chloroform were prepared separately and the PC solution was added to the conducting filler solution at different proportions. The mixed solutions were subjected to magnetic stirring for 2 h. The solvent was then removed by evaporation under vacuum at room temperature to get the PPPC blends.

Characterization Techniques

Fourier transform infrared (FTIR) measurements were made with a fully computerized Nicolet impact 400D FTIR spectrophotometer. Polymers were mixed thoroughly with potassium bromide and compressed into pellets before recording.

Electrical conductivity (σ_{dc}) of films was measured using the standard spring-loaded pressure contact four probe conductivity meter supplied by Keithley, Bangalore, India with 6221 direct current (DC) and AC current source and 2182A nanovoltmeter. The conductivity (σ_0) was calculated using the relationship $\sigma_0 = (\ln 2/\pi d)\ (I/V)$, where d is the thickness of the film, I is the current, and V is the voltage. A constant current was passed with a direct current (DC) voltage source through two outer electrodes and an output voltage was measured across the inner electrodes with the voltmeter. The small uniform sized 11 mm disk sample was placed in a PID-controlled oven before the measurement.

Polarized light micrographs (PLMs) were taken in an Olympus BX 51 microscope after drop casting the solution of sample in a clean dry glass plate. For scanning electron microscopy (SEM) measurements, samples were subjected for thin gold coating using a JEOL JFC-1200 fine coater. The probing side was inserted into JEOL JSM-5600 LV scanning electron microscope for taking photographs. Atomic force microscopy (AFM) images were recorded under ambient conditions using Ntegra multimode Nanoscope IV operating in the tapping mode regime. Microfabricated silicon cantilever tips (MPP-11100-10) with a resonance frequency of 284–299 kHz and a spring constant of 20–80 Nm^{-1} were used. The scan rate varied from 0.5 to 1.5 Hz.

Rheological properties of the conductive blends were measured using Modulated Compact Rheometre-150 Physica (Germany) in dynamic oscillatory mode at 100°C (frequency range, 0.001–1000 rad/s). In all the rheological tests, the parallel plate sensor with a diameter of 50 mm and a gap size of 0.25 mm was used.

Thermal stability measurements were performed at a heating rate of 10°C/min in nitrogen atmosphere using Shimadzu,

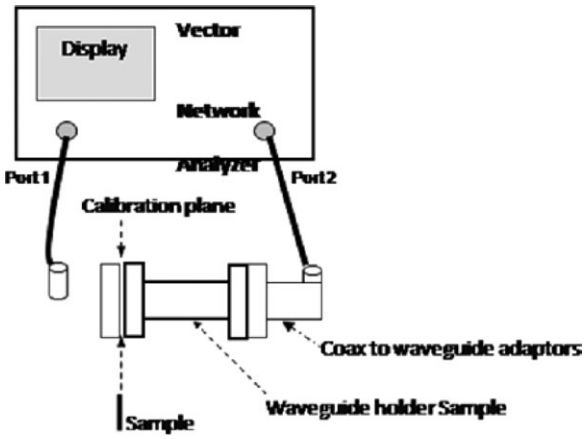

Figure 1. Experimental set up for the measurement of EMI SE.

DTG-60 equipment. Differential scanning calorimetry (DSC) scans were performed using Dupont DSC 2010 differential scanning calorimeter attached to Thermal Analyst 2100 data solution under nitrogen atmosphere at a heating rate of 10°C/min.

Tensile tests of the PC and PPIC composites were conducted using dumb-bell-shaped samples of width 4 mm and thickness in the range 1.5–2 mm. The measurements were carried out in an Instron universal testing machine. HTE-5KN Load cell is used and calibration was performed as per the ASTM procedure D 638 at a crosshead speed of 2 mm/min at room temperature. EMI SE of the prepared samples have been measured using a laboratory developed one-port coaxial sample holder backed by metallic plate as short circuit on Vector network analyzer (VNA), Wiltron 37247B in the desired frequency range. The reference value of return loss (RL) in dB was measured by connecting the one-port sample holder at the test port without sample on the calibrated VNA. Now, the sample is inserted in the holder and the RL value is recorded. The difference between these two values is the measured RL of the inserted sample. Half of this measured RL is the EMI SE of the sample in dB. In a similar fashion, the EMI SE measurements of other samples were performed by replacing the previous sample. The SE was measured using an X-band waveguide as a sample holder (Figure 1). Samples having a thickness of 2 mm were used during measurement. The EMI shielding measurement was carried out for each sample by continuously sweeping the frequency between 2 and 8 GHz.

RESULTS AND DISCUSSION

Nanostructured electromagnetic PPIC was prepared by the oxidative emulsion polymerization of anilinium salt of PDPSA as reported in the experimental section. The conducting state of PPIC was characterized by recording the UV–visible spectra and it exhibited a prominent peak at 430 nm and a free carrier tail around 780 nm corresponding to the polaron band (conducting state). Electrical conductivity measurements of PPIC showed a value of the order of 1 S/cm and the magnetic property measurements carried out using vibrating sample magnetometer exhibited a saturation magnetization of ~ 2.5 emu/g with a coercive force of 50 Oe. Particle size measurement of PPIC was carried out using dynamic light scattering technique which exhibited diameter in the range of 50–150 nm.

Table I. Electrical Conductivity and Mechanical Strength of PPPC Blends as a Function of the PPIC Content

Sample	weight of PPIC in PPPC (%)	Electrical conductivity (S/cm)	Tensile strength (MPa)	Elongation at break (%)
PC	0	5×10^{-12}	57	130
PPPC1	2	4×10^{-8}	57.18	132
PPPC2	3	6×10^{-7}	58.1	132
PPPC3	4	7.3×10^{-6}	58.2	135
PPPC4	5	2.4×10^{-4}	58.5	136
PPPC5	6	7.5×10^{-4}	57.7	136
PPPC6	7	9.5×10^{-3}	57.5	135
PPPC7	10	1.6×10^{-2}	57.3	134
PPPC8	20	1.6×10^{-2}	57.1	133
PPPC9	30	1.6×10^{-2}	58.1	132

Composite of PPPCs was prepared with varying ratios of PPIC to PC. The PPPC composites with 2, 3 ,4, 5, 6, 7, 10, 20 and 30 weight % of PPIC were designated as PPPC1, PPPC2, PPPC3, PPPC4, PPPC5, PPPC6, PPPC7, PPPC8 and PPPC9, respectively, and is summarized in Table I. Visual inspection of the PPPC blends showed transparent emeraldine green-colored film whose intensity increased with the PPIC concentration. A representative film of PPPC is shown in Figure 2.

FTIR Spectroscopy

Generally, most of the bands of PC and PPPC in FTIR spectra overlap as shown in Figure 3. The band at 1770 cm^{-1} in the spectrum of PC shifted to a lower frequency by about 8 cm^{-1} in PPPC and is observed to slightly bifurcate, confirming the

Figure 2. Clear transparent green film of PPPC blend. [Color figure can be viewed in the online issue, which is available at wileyonlinelibrary.com.]

Applied Polymer SCIENCE

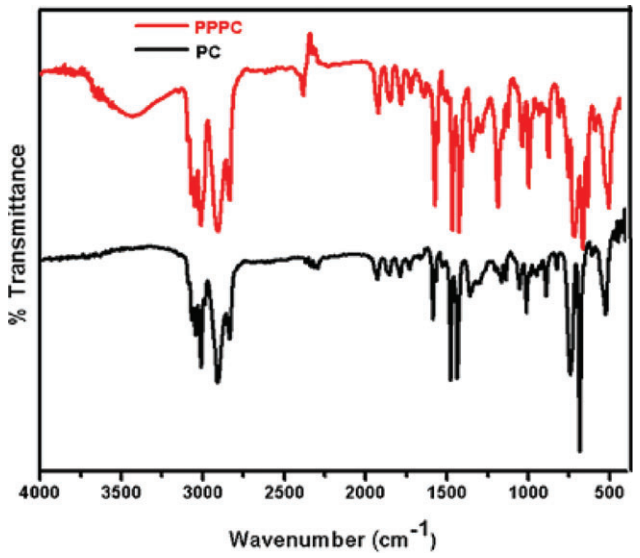

Figure 3. FTIR spectra of PC and PPPC. [Color figure can be viewed in the online issue, which is available at wileyonlinelibrary.com.]

hydrogen bonding interaction existing between NH of polyaniline and C=O of PC as shown in Scheme 1.[18]

Electrical Conductivity and Conduction Mechanism

Electrical conductivity is the most sensitive method to monitor the continuity of the conductive filler phase within the host matrix. The particular concentration at which there is sharp increase in conductivity can be termed as percolation threshold concentration.[19] The low value of percolation threshold is an important criterion in the preparation of the conductive blend of polyaniline and insulating polymer as to minimize processing problems and depletion of the mechanical properties of the host-insulating polymer. Table I summarizes the conductivity values corresponding to the various composition of the blend. PC is an insulative polymer having conductivity of 10^{-12} S/cm. It was observed that the electrical conductivity can be controlled in a wide range by changing the amount of conducting PPIC. Electrical conductivity of PPPC increased to 4×10^{-8}, 6×10^{-7}, 7.3×10^{-6}, 2.4×10^{-4}, 7.5×10^{-4}, 9.5×10^{-3}, 1.6×10^{-2} S/cm in PPPC1 PPPC2, PPPC3, PPPC4, PPPC5, PPPC6, PPPC7, respectively. Such an unpredictable enhancement in electrical conductivity at the threshold concentration was explained by the formation of percolated structure of PPIC in PPPC. The percolation threshold concentration curve PPIC in PPPC is shown in Figure 4. This can be taken as the point where the material changes from insulating phase to conducting

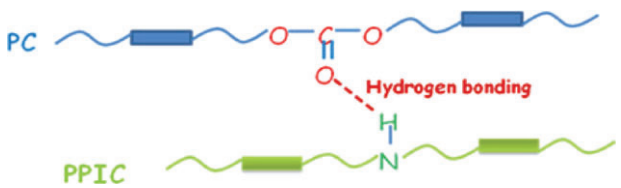

Scheme 1. Hydrogen bonding between PC and PPIC. [Color figure can be viewed in the online issue, which is available at wileyonlinelibrary.com.]

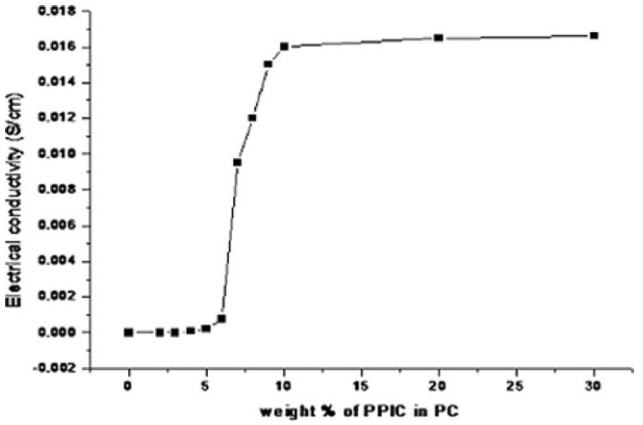

Figure 4. Percolation threshold concentration curve of PPIC in PPPC.

phase. At the threshold concentration, the isolated conducting PPIC in the PC matrix is bridged by a conducting channel of PPIC, forming an interconnected network, which results in the abrupt increase in conductivity and thus generating continuous conducting paths. Onset of percolation is further strengthened by the morphological observation under PLM,SEM and AFM.

To study the electronic transport behavior of the material, the conductivity of the materials as a function of temperature was measured over the temperature range of 303–393 K and is as shown in Figure 6. The conductivity initially increased with increasing temperature and then decreased and this is typical for semiconductors.

According to Arrhenius equation,

$$\rho = \rho_0 \exp\left[\left(\frac{E_a}{kT}\right)\right] \quad (1)$$

where E_a is the thermal activation energy during polaron conduction and ρ_o is a parameter depending on the semiconductor

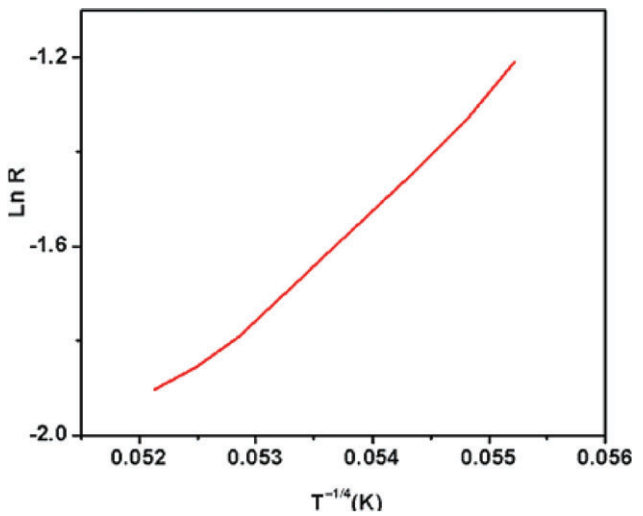

Figure 5. Temperature-dependent conductivity of PPPC blend. [Color figure can be viewed in the online issue, which is available at wileyonlinelibrary.com.]

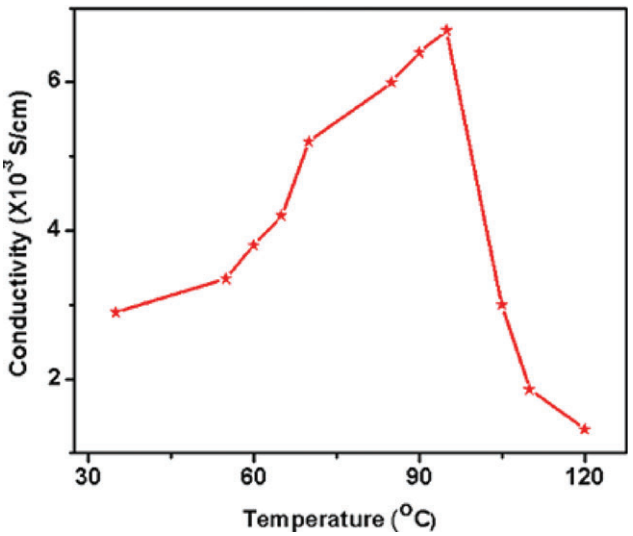

Figure 6. 3D VRH plot of PPPC blend. [Color figure can be viewed in the online issue, which is available at wileyonlinelibrary.com.]

nature. Arrhenius plot of the measured conductivity (ρ vs. $1/T$) was made. It was observed that the curve is deviating from straight line and therefore deviates from Arrhenius equation which is typical for simple semiconductors. But it has been observed that the data are fitting with variable VRH of localized polarons according to eq. (2)

$$R_{(T)} = R_o \exp(T_o/T)^m \quad (2)$$

where $R_{(T)}$ is the resistivity, R_o is the pre-exponential factor, and T_o is the Mott characteristic temperature.[20]

T_o can be obtained from the slope of ln $R_{(T)}$ vs. T^{-m} plot. The value of the exponent "m" depends critically on the nature of hopping process. The exponent $m = 1/4$, 1/3, and1/2 for 3D, 2D, and 1D hopping, respectively. To obtain the value of "m" with more accuracy, a plot was made with ln ρ vs. $T^{-1/m,}$ where $m = 1/4$, 1/3, and 1/2 and the best fit was obtained for $m = 1/4$ and the plot of ln ρ vs. $T^{-1/4}$ is shown in Figure 5. The plot showed a linear trend and therefore followed 3D-VRH model. T_o values derived from the slope were found to be 226 K.

Morphology of PPPC

Morphology of PPPCs was studied for monitoring the onset of percolation threshold concentration and also checking the compatibility of the components PC and PPIC. Figure 7 shows the PLM photographs at a magnification of 20× of PPPC blends with different percentage loadings of PPIC. The PLM image of PPPC1 with 5 wt % loading of PPIC is shown in Figure 7(a). In the micrograph, the dispersed phase of PPIC appears to exist as isolated globules which are mostly surrounded by the insulating matrix and are therefore unable to come into contact with each other. On increasing the concentration of PPIC to 10 wt %, it exhibited a percolated structure [Figure 7(b)]. On further increase in PPIC to 15 wt %, it exhibited thick network structure [Figure 7(c)] and tend to form organized aggregates of fibrillar morphology. The onset of percolation of PPIC in PPPC blend was further studied by observation under SEM and AFM Figure 8(a, b) shows the SEM and AFM micrographs of PPPC containing 10 wt % of PPIC. The observation made was complementary to that obtained from PLM. Both SEM and AFM photographs showed conductive network of PPIC containing nanostructured electromagnetic PPIC and it was observed that the conductive phase is fluidized and there is connectivity between the conductive chains and the interconnectivity (percolation) is observed between the conducting phases. Bright portion in the micrograph indicated the presence of electromagnetic filler and black portion, the matrix polymer.

Rheological Properties

The presence of exfoliated nanoclay and the interaction between the conductive filler host matrix was manifested from the rheological property measurements. The dynamic oscillatory measurements of the conductive blends were carried out under angular frequency sweep. Loss modulus (G'') and storage modulus (G') were measured as a function of frequency at 170°C under angular sweep of 1–100 rad/s at 5% strain and is shown in Figure 9. The G' is related to the ability of the material to store energy when an oscillatory force is applied to the specimen and the G'' is related to the ability to dissipate the energy. These properties were measured to examine the degree of filler–host matrix interaction in the conductive film. Solid-like behavior ($G' > G''$) could be observed from the dynamic oscillatory responses. The G'-values of PC and PPPC measured at 10 rad/s are 10.9 and 15 KPa, respectively. PPPC showed enhanced storage modulus on comparing with PC. This increased storage modulus observed might be arising owing to the interaction between the PPIC and the PC. It may be observed from the plot that the values of the frequency at the intersection of G' and G'' vs. angular frequency curve, the film of PPPC showed

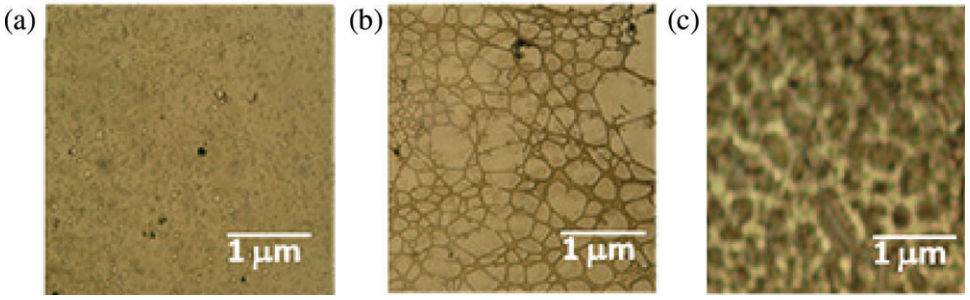

Figure 7. Polarized light micrographs of (a) 5% PPIC, (b) 10% PPIC, and (c) 15% PPIC blends showing the percolation network formation. [Color figure can be viewed in the online issue, which is available at wileyonlinelibrary.com.]

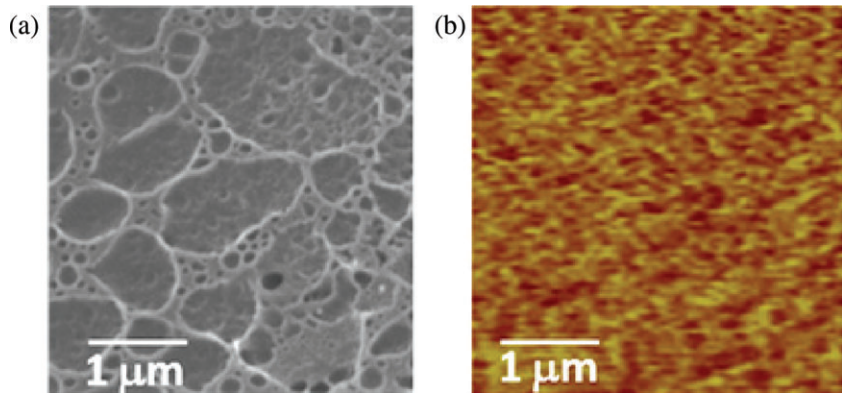

Figure 8. (a) SEM and (b) AFM figures of PPPC blend at 10 wt % of PPIC. [Color figure can be viewed in the online issue, which is available at wileyonlinelibrary.com.]

value of 2.06 rad/s which is obviously lower than that of the frequency observed for neat PC. This may be owing to the dramatic exfoliation of clay into nanometer scale and also owing to the interaction between the nanoclay layers and the primary particles contributing to shear thinning as reported by Acierno and coworkers.[21]

Thermal Stability

Thermal stability of PPPC and PC was studied by thermogravimetry (TGA) and is shown in Figure 10. Both PPPC and PC showed a small weight loss below 100°C presumably caused by the loss of solvent and low-molecular-weight volatile impurities. The second stage weight loss occurs at 411°C in PC corresponding to the decomposition of the polymer. In PPPC, the decomposition temperature was observed at 422°C. The higher decomposition temperature observed for PPPC compared to PC can be owing to the hydrogen bonding interaction existing between PPIC and PC and also owing to the presence of nanoclay particles with high aspect ratio which may hinder the degradation process providing a barrier to preclude evaporation of small molecules generated during the thermal decomposition process. According to Zanetti and Pereira,[22] the barrier effect of the clay increases during volatilization because of the reassembly of the silicate layers occurring on the polymer surface during the thermal decomposition. TG of PPPC showed a residual char content at 600°C corresponding to the residue of clay present in the system. Thermal phase transition temperature of PC and PPPC was studied by DSC and is shown in Figure 11. PC exhibited a peak at 145°C which corresponds to its glass transition temperature (T_g). PC exhibited another endothermic peak at around 418°C corresponding to the decomposition of the same and is matching with the TG data, whereas DSC curve of PPPC showed T_g at 110°C and decomposition at 426°C.

Mechanical Testing

Mechanical properties of the conductive composites were measured with uniform size strips of conductive film as per the ASTM standard procedure. Effect of amount of conductive filler on the ultimate tensile strength (UTS) was measured and is summarized in Table I. PC showed UTS of 57 MPa and elongation at break at 28%. Generally, the UTS and elongation at

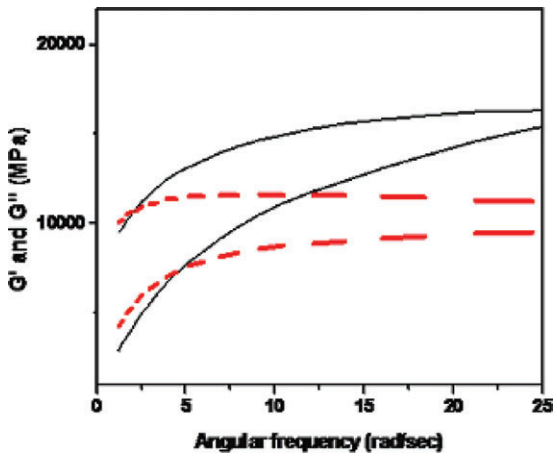

Figure 9. Plot of storage modulus and loss modulus vs. angular frequency (· · · PPPC (G') and PC (G') and - - - PPPC (G'') and PC (G'')). [Color figure can be viewed in the online issue, which is available at wileyonlinelibrary.com.]

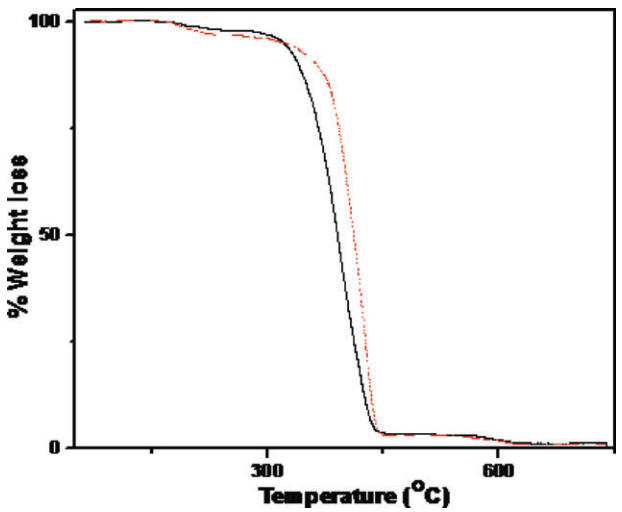

Figure 10. TGA plots of · · · PC and - - - PPPC blend. [Color figure can be viewed in the online issue, which is available at wileyonlinelibrary.com.]

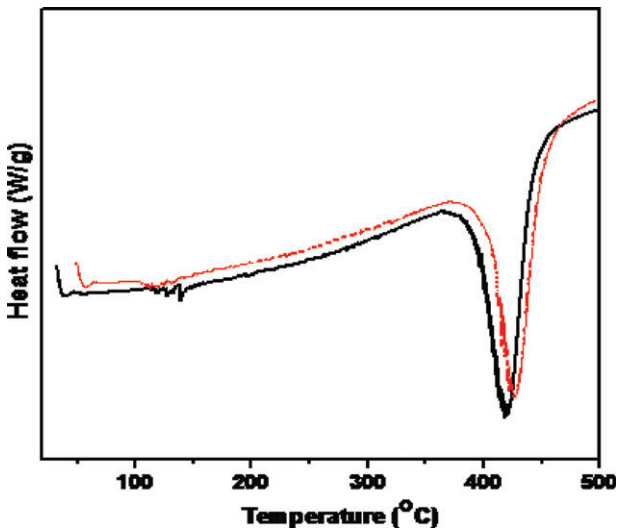

Figure 11. DSC plots of · · · PC and - - - PPPC blend. [Color figure can be viewed in the online issue, which is available at wileyonlinelibrary.com.]

break decreased by the addition of conductive fillers, indicating that the conductive components are slightly incompatible with the PC matrix despite the nature of the counter ion used for the protonation. But the UTS and elongation at break of these PPPC films showed positive variation for conductive films containing 5, 10, 15, 20, 25, and 30% of PPIC. It exhibited UTS and elongation at break of 57.18 (130%), 58.1 (131%), 58.2 (132%), 58.5(132%), 58.7(133%), and 58.9 (134%), respectively. The higher value observed for nanocomposites is owing to the presence of exfoliated nanoclay having high aspect ratio and also owing to the excellent compatibility induced by the amphiphilic dopant.[23]

EMI Shielding

EMI SE of the conductive films was measured as per the standard procedure.[24] EMI SE can be taken as the ratio of the field strength before and after attenuation. It was observed that as the amount of filler loading was increased, SE also increased. When irradiated with electromagnetic radiation of 8 GHz, the SE of conductive films was measured to have values: 24 dB (5% PPICSA), 42 dB (10%), 50 dB (15%), and 52 dB (30%), respectively. Generally, the EMI SE measurement showed similar trends for all the conductive fillers. The conductive films containing PPIC can attenuate electromagnetic radiation by three mechanisms of absorption, reflection, and multiple reflections. Absorption loss is caused by the heat loss under the action between magnetic and electric dipole present in the shielding material and the electromagnetic field. Reflection owing to the magnetic polyhydroxy iron species and the multiple reflection loss as a result of the presence of porous/multiple-layered clay present in the shielding material which contribute large surface/interface area for multiple reflections. The higher the SE value, the less energy passes through the sample. The results revealed that the conductive blends under investigation can be considered as a prospective candidate for the encapsulation of microelectronic devices as a shielding material.[25]

CONCLUSIONS

We have successfully developed EMI shielding material from the conductive composite of PC and nanostructured electromagnetic PPIC composite. The onset of percolation threshold concentration was manifested from the studies made from electrical conductivity measurements in combination with morphology. Electrical conduction mechanism in PPPC studied by measuring temperature-dependent conductivity was found to be following 3D VRH. The superior rheological properties exhibited by conductive blends containing clay nanocomposites can be explained owing to the presence of the nanoclay primary particles and the strong interfacial interactions between the doped PPIC and the clay platelets present. EMI SE and thermomechanical measurements suggest that these materials can be used as a prospectable candidate for the encapsulation of electronic devices for civil applications.

ACKNOWLEDGMENTS

The authors thank the Indian Space Research Organisation for their financial support from project GAP 109439 and NWP 23 (Net work project). The authors are also thankful to Mr. M. R. Chandran, NIIST Trivandrum, for SEM analysis. Mr. Kamalesh Patel, NPL, New Delhi, for EMI SE measurements, Dr. Roy Joseph, SCTIMST, Trivandrum for tensile strength measurements. V.L. Reena thanks CSIR-New Delhi, India, for the senior research fellowship.

REFERENCES

1. Kim, B. R.; Lee, H. K.; Park, S. H.; Kim, H. K. *Thin Solid Films* **2011,** *519*, 3492.
2. Yang, Y.; Gupta, M. C.; Dudley, K. L.; Lawrence, R. W. *Nano Lett.* **2005,** *5*, 2131.
3. Zhu, J.; Wei, S.; Zhang, L.; Mao, Y.; Ryu, J.; Karki, A. B.; Young, D. P.; Guo, Z. *J. Mater. Chem.* **2011,** *21*, 342.
4. Zhu, J.; Wei, S.; Zhang, L.; Mao, Y.; Ryu, J.; Mavinakuli, P.; Karki, A. B.; Young, D. P.; Guo, Z. *J. Phys. Chem. C* **2010,** *114*, 16335.
5. Li, X.; Wan, M.; Wei, Y.; Shen, J.; Chen, Z. *J. Phys. Chem. B* **2006,** *110*, 14623.
6. Sudha, J. D.; Sivakala, S.; Prasanth, R.; Reena, V. L.; Radhakrishnan Nair, P. *Comp. Sci. Technol.* **2009,** *69*, 358.
7. Cao, Y.; Paul, S.; Heeger, A. J. *Synth. Met.* **1992,** *48*, 91.
8. Pud, A.; Ogurtsov, N.; Korzhenko, A.; Shapoval, G. *Prog. Polym. Sci.* **2003,** *28*, 1701.
9. Sudha, J. D.; Sivakala, S.; Kamalesh Patel; Radhakrishnan Nair, P. *Comp. A* **2010,** *41*, 1647.
10. Sudha, J. D.; Reena, V. L.; Pavithran, C. *J. Polym. Sci. B Polym. Phys.* **2007,** *45*, 2664.
11. Paul, R. K.; Pillai, C. K. S. *Synth. Metal* **2000,** *27*, 109.
12. Cao, Y.; Smith, P.; Heeger, A. J. *Synth. Met.* **1993,** *57*, 3514.
13. Heeger, A. J. *Synth. Met.* **1993,** *57*, 3471.
14. Jeevananda, T.; Siddaramaiah; Annadurai, V.; Somashekar, R. *J. Appl. Polym. Sci.* **2001,** *82*, 383.

15. Wang, H. L.; Toppare, L.; Fernandez, J. E. *Macromolecules* **1990,** *23*, 1053.
16. Roy, R.; Bhattacharyya, A.; Sen, S. K.; Sen, S. *Phys. Stat. Sol.* **1998,** *165*, 245.
17. Lee, W. J.; Kim Y. J.; Kaang, S. *Synth. Met.* **2000,***113*, 237.
18. Reena, V. L.; Sudha, J. D.; Pavithran, C. *J. Phys. Chem. B* **2010,** *114*, 2578.
19. Yan, Y. L.; Gupta, M. C.; Dudley, K. L.; Lawrence, R. W. *J. Nanosci. Nanotechnol.* **2005,** *5*, 927.
20. Mott, N. F. *Rev. Mod. Phys.* **1978,** *50*, 203.
21. Filippone, G.; Dintcheva, N.; Acierno, D.; La Mantia, F. P. *Polymer* **2008,** *49*, 1312.
22. Zanetti, S. M.; Pereira, M. G. S. *J. Eur. Ceram. Soc.* **2007,** *27*, 3647.
23. Guilherme, M.; Barra, O.; Leyva, M. E.; Soares, B. G.; Mattoso l. H.; Sens, M. *J. Appl. Polym. Sci.* **2001,** *82*, 114.
24. Wang, Y.; Jing, X. *Polym. Adv. Technol.* **2005,** *16*, 344.
25. Kaynak, A. *Mater. Res. Bull.* **1996,** *31*, 845.